Earth's Future

RESEARCH ARTICLE
10.1029/2019EF001394

Key Points:

- The shortest Pacific to Atlantic connectivity timescale is >2 years, so tipping point for a species requiring single-summer transit is highly improbable
- Advective pathway associated with shortest connectivity timescales is via Barrow Canyon and Canadian Archipelago, but is only sporadically available
- A sporadically available pathway was linked to the anomalously cyclonic Arctic

Correspondence to:
S. J. Kelly,
stephen.kelly@noc.ac.uk

Citation:
Kelly, S. J., Popova, E., Aksenov, Y., Marsh, R., & Yool, A. (2020). They came from the Pacific: How changing Arctic currents could contribute to an ecological regime shift in the Atlantic Ocean. *Earth's Future*, *8*, e2019EF001394. https://doi.org/10.1029/2019EF001394

Received 18 OCT 2019
Accepted 28 JAN 2020
Accepted article online 5 FEB 2020

They Came From the Pacific: How Changing Arctic Currents Could Contribute to an Ecological Regime Shift in the Atlantic Ocean

S. J. Kelly[1,2], E. Popova[1], Y. Aksenov[1], R. Marsh[2], and A. Yool[1]

[1]National Oceanography Centre, Southampton, UK, [2]Ocean and Earth Science, University of Southampton, Southampton, UK

Abstract The Arctic Ocean is rapidly changing. With warming waters, receding sea ice, and changing circulation patterns, it has been hypothesized that previously closed ecological pathways between the Pacific and Atlantic Oceans will be opened as we move toward a seasonally ice-free Arctic. The discovery of the Pacific diatom *Neodenticula seminae* in the Atlantic suggests that a tipping point may have already been reached and this "opening up" of the Arctic could already be underway. Here, we investigate how circulation connectivity between the Pacific and Atlantic Oceans has changed in recent decades, using a state-of-the-art high-resolution ocean model and a Lagrangian particle-tracking method. We identify four main trans-Arctic pathways and a fifth route that is sporadically available with a shorter connectivity timescale. We discuss potential explanations for the existence of this "shortcut" advective pathway, linking it to a shift in atmospheric and oceanic circulation regimes. Advective timescales associated with each route are quantified, and seasonal and interannual trends in the main four pathways are discussed, including an increase in Fram Strait outflow relative to the Canadian Archipelago. In conclusion, we note that while tipping points for ecological connectivity are species dependent, even the most direct routes require multiannual connectivity timescales.

Plain Language Summary With a warming Arctic Ocean, it has been suggested that the ocean currents that connect the Pacific to the Atlantic may change. This could have potential biological consequences, including bringing Pacific species of plankton to the Atlantic. We investigate how the pathways bringing Pacific water to the Atlantic have changed, identify a pathway that takes less time that other routes to bring waters from Pacific to the Atlantic (but that is only occasionally available), and note that even the shortest timescales are over 2 years.

1. Introduction

1.1. Marine Ecological Connectivity

The term "marine ecological connectivity" is used to describe the exchange of individual organisms within and between distinct subpopulations within the ocean (Cowen et al., 2006; Cowen & Sponaugle, 2009).

Ecological connectivity aims to explain how different ecosystems are linked in time and space, describing which subpopulations are sources of biota for other regions, sinks for biota from elsewhere, or whether a two-way exchange takes place. This is an inherently interdisciplinary problem linking the biology and physics of the oceans and is influenced by both the circulation of the ocean and the biological characteristics of the species themselves (Cowen & Sponaugle, 2009).

Marine ecological connectivity can be broadly split into (passive) circulation connectivity and active migratory connectivity (Popova et al., 2019). Circulation connectivity describes the advective pathways along which ocean currents transport waters from one region to another (Van Gennip et al., 2017), whereas active migratory connectivity is driven directly by species themselves swimming between one region and another for breeding and feeding (Webster et al., 2002). The two are not fully independent of each other—even marine species which are capable of active migration as adults typically have a planktonic stage earlier in their life cycles (Selkoe & Toonen, 2011). However, as a large number of marine species are not capable of active migration, and because of the additional complexity of active migration (drivers and locomotion), we focus on passive circulation connectivity in this study.

In addition to understanding how different regions are connected spatially, it is important to understand how they are connected in time: specifically, their connectivity timescales. From a purely oceanographic point of view, one part of the ocean may be connected to another by circulation pathways, but this does not automatically imply that ecological connectivity between the two places exists. When considering marine ecosystems, the timescales on which different regions are linked becomes important to describe whether or not different regions are ecologically connected by ocean currents (Jönsson & Watson, 2016).

The timescales required to allow for ecological connectivity vary depending on the context of the problem. For species with a planktonic stage early in their life cycle, their pelagic larval duration (PLD) can be used as a proxy for the timescale required for a source location to be ecologically connected to a sink location during that part of its life cycle (Selkoe & Toonen, 2011; Shanks, 2009). PLD can be the key limiting factor in describing the ecological connectivity—for example, in the case of corals, which are dispersed entirely during their pelagic larval stages but remain static throughout their adult lives (Mayorga-Adame et al., 2017). However, for fish and other species with an active migratory adult stage, passive circulation connectivity during the PLD provides only part of the story and is limited to describing their connectivity during that planktonic stage.

PLD varies highly between species (Bradford et al., 2015; Van Herwerden et al., 2006), but it is not the only limiting factor when considering connectivity timescales. Other barriers to connectivity exist, including the survival of the larvae as it is transported from source to sink (Treml et al., 2012). For larvae and plankton, limiting factors can include temperature, the availability of food, and predation (Cowen & Sponaugle, 2009), as well as access to nutrients and sunlight in the case of phytoplankton (Arteaga et al., 2014). For a source to be ecologically connected to a sink, it is essential that the connectivity timescale and conditions encountered along the route allow for the species to reach the sink alive.

These biophysical limitations, which are species specific, as well as changes in strength and direction of purely oceanic connectivity pathways (van Gennip et al., 2017), provide the limits as to whether or not one region is ecologically connected to another. Here, we investigate the connectivity pathways and timescales linking the North Pacific (source) to the North Atlantic (sink) across the Arctic and discuss the implications of potentially increased ecological connectivity between the two regions as the Arctic changes.

1.2. Motivation: Changing Trans-Arctic Connectivity

Sea ice cover in the Arctic Ocean has declined significantly over recent decades due to anthropogenic climate change (Overland & Wang, 2013). It has been hypothesized that this reduction in sea ice is causing an acceleration of Arctic surface currents (e.g., Armitage et al., 2017), which in turn is causing accelerated Pacific-Atlantic connectivity, with potential biological consequences such as nonnative species colonizing the Atlantic Ocean (Reid et al., 2007).

Increased circulation connectivity (Popova et al., 2019) between the North Pacific and the North Atlantic could lead to the enhanced ecological connectivity between their ecosystems in ways that previously have not been possible (Reid et al., 2007). This makes understanding the consequences of acceleration in Arctic currents for ecological connectivity important.

One of the striking examples of increased ecological connectivity between these basins is the recent Atlantic appearance of the Pacific diatom, *Neodenticula seminae* (Reid et al., 2007). This species was observed by a Continuous Plankton Recorder (CPR) survey in the Atlantic Ocean in 1999, seemingly its first occurrence in the Atlantic for millennia, and Reid et al. (2007) proposed accelerated connectivity due to reduced sea ice cover as an explanation. Subsequent analysis of sediment cores has suggested that, although not found in any CPR surveys prior to 1999, the species may in fact have been present in the Fram Strait as early as 1989 (Matul et al., 2018).

Since its initial recording in the Labrador Sea in 1999, *N. seminae* has established itself in the North Atlantic, blooming in several locations since (Miettinen et al., 2013; Reid et al., 2007), and it has been suggested that trans-Arctic connectivity responsible for *N. seminae*'s arrival may either still be active or even accelerated in more recent years (Miettinen et al., 2013). This provides motivation for this research: If Pacific to Atlantic connectivity has changed, it is important to understand how, in order to better understand the potential for future trans-Arctic migrations of species previously endemic to the two basins.

N. seminae is not the only example of trans-Arctic migration of Pacific-native species to the North Atlantic. *Mytilus trossulus* is a species of mussel extant in the North Pacific, North Atlantic, and Arctic Ocean with a planktonic period of 2 weeks to 3 months (Yaroslavtseva & Sergeeva, 2006). A population of the species around northern and north-western Greenland was analyzed and found to be more genetically similar to populations in the Pacific than the rest of the Atlantic, leading the authors to suggest that Pacific to Atlantic transport of mussels is already sporadically taking place, given favorable climate and hydrodynamic events (Bach et al., 2019).

It has been predicted that an "opening up" of the Arctic gateway could result in at least 35% (77 of 219) of shallow water mollusk species native to the northern Bering Sea becoming established in the North Atlantic Ocean without direct human aid (Vermeij & Roopnarine, 2008). Other research suggests that Pacific to Atlantic "invasions" will include species at higher trophic levels, including fish (Wisz et al., 2015). Adult species are described by active ecological connectivity, but they have a pelagic larval stage earlier in their life cycles where they are distributed by ocean currents. How long this stage lasts is defined by their PLD, which can be as short as 2–4 weeks for some species of mackerel (van Herwerden et al., 2006) or as long as 1.5 years for rock lobsters (Bradford et al., 2015).

Assessing the ecological impacts of nonnative species establishing populations in the North Atlantic is a complex question to address. While extinctions of preexisting species as a result of marine invasions are uncommon (Vermeij & Roopnarine, 2008), other possible consequences include hybridization of existing species and increased competition for resources with Pacific-native species (Vermeij & Roopnarine, 2008).

In order to understand the potential impacts of nonnative species reaching the Atlantic Ocean, it is necessary to understand how they manage to traverse the Arctic Ocean. To address this, we focus on answering the question of how passive ecological connectivity between the Pacific and Atlantic oceans has changed in recent decades.

The large-scale advective pathways of the Arctic Ocean are well described (Aksenov et al., 2011, 2016; Wassmann et al., 2015), and it is known that Pacific waters reach the Atlantic via the Arctic. Key pathways are highlighted here in Figure 1. Three main Pacific inflow pathways are shown, through Barrow Canyon, Herald Canyon, and a central channel between the two that flows via Herald and Hana shoals (Aksenov et al., 2016; Lin et al., 2016; Timmermans et al., 2014). The anticyclonic Beaufort Gyre is the dominant surface feature in the western Arctic (Proshutinsky et al., 2002), and the transpolar drift transports water from Siberia toward the Atlantic Ocean (Steele et al., 2004). Water exits the Arctic through one of two pathways: either via Fram Strait, where the East Greenland Current brings it to the Atlantic (Bacon et al., 2014), or it reaches the Atlantic via one of many possible routes through the Canadian Archipelago (Rudels, 2015).

However, climate change is altering Arctic advection and connectivity pathways, and this is believed to be the driver behind Pacific species reaching the Atlantic (Reid et al., 2007). There are several ways that trans-Arctic connectivity could change to make "invasions" of nonnative species more likely. One such mechanism is an acceleration of currents across the Arctic (Armitage et al., 2017). As the Artic is a harsh environment for subpolar species, minimizing transit times across it increases the likelihood of planktonic species surviving the journey.

We hypothesize that any increased circulation-based ecological connectivity is not as simple as accelerating Arctic currents in general and that three possible changes (or their combinations) could be involved. In addition to an acceleration of Arctic currents, it is possible that connectivity timescales could be reduced by shifting advective pathways, or even opening up of new ones. Finally, it is also possible that the changed conditions in a warmer, more ice-free Arctic could play a key role in making existing, but previously nonviable, advective pathways survivable.

We suggest the following three hypotheses (or some combination of them) as explanations for how Pacific species could reach the Atlantic Ocean:

- Acceleration of surface currents
- Changing of dominant trans-Arctic advective pathways and/or appearance of new/faster trans-Arctic routes

- Changes to ecologically important properties along the routes (e.g., temperature and availability of light/nutrients)

Additionally, we note that nonoceanographic changes could be responsible for invasive species traversing the Arctic. Specifically, ballast water has been invoked as a potential explanation for successful long-range colonization events in the Arctic (Reid et al., 2007) and elsewhere (Smith et al., 2018). Reid et al. (2007) discuss this possibility as a potential explanation for the appearance of *N. seminae* but argue against it on the basis of the limited amount of trans-Arctic shipping that took place in the 1990s, coupled with the fact that any alternative shipping route would require the subpolar diatoms to survive tropical conditions, which the authors concluded was highly unlikely. However, with trans-Arctic shipping likely to increase as a consequence of reduced sea ice in the region (Aksenov et al., 2017; Østreng et al., 2013), this must be noted as another indirect way in which a changing Arctic could facilitate an ecological regime shift in the North Atlantic in the future.

Here, we aim to address the first two of these hypotheses by analyzing output from a 1/12° NEMO ocean model (specifically, ORCA0083-N006) from a Lagrangian perspective. As we are motivated by understanding potential biological consequences of changing connectivity, we focus primarily on investigating the advective pathways with the shortest connectivity timescales.

2. Methods

2.1. NEMO Model and ARIANE Particle Tracking

For the experiments in this paper, we used the NEMO model (NEMO stands for Nucleus for European Modeling of the Ocean framework) in conjunction with the ARIANE Lagrangian analysis tool. We utilized presaved 5-day mean output from the 1/12° resolution ORCA0083-N006 configuration of NEMO (Madec, 2014). This version of NEMO has approximately 3- to 5-km horizontal resolution in the Arctic Ocean and 75 vertical depth layers (31 levels between the surface and 200-m depth) and was run coupled to the Louvian-la-Neuve Ice Model (LIM2) (Fichefet, & Maqueda, M. a. M., 1997; Goosse & Fichefet, 1999). At the time of writing, this was the highest resolution version of NEMO available, with horizontal resolution sufficient for it to be eddy-resolving throughout much of the Arctic Ocean, though only eddy-permitting on the shelves due to their small Rossby radii (Nurser & Bacon, 2014).

The configuration of NEMO used here was forced with version 5.2 of the DRAKKAR forcing set (DFS) (Brodeau et al., 2010). DFS 5.2 is based on ERA40 reanalysis data, comprising of 6-hourly means for wind, humidity, and atmospheric temperature, daily means for radiative fluxes (both longwave and shortwave), and monthly means for precipitation. A monthly climatology is used for river runoff, taken from CORE2 reanalysis (Brodeau et al., 2010; Timmermann et al., 2005). The model hindcast used in these experiments was created using this forcing set for the period 1958–2015.

NEMO has been extensively validated throughout the Arctic. Kelly et al. (2018) investigated how well NEMO reproduced sea ice coverage and how the modeled SSH and barotropic streamfunction compared to satellite measurements (Armitage et al., 2016). This was expanded upon in Kelly et al. (2019), where the modeled mixed layer was validated against observational data (Peralta-Ferriz & Woodgate, 2015) and good model skill was found. Similar configurations of NEMO have been further validated, with modeled water mass types and stratification found to be in agreement with observations (Aksenov et al., 2016; Janout et al., 2015; Luneva et al., 2015).

Here, we use the ARIANE (Blanke & Raynaud, 1997) Lagrangian particle-tracking tool to analyze output from the NEMO model. This software works by reading in the (precalculated) 5-day mean output from the NEMO model and using it to advect virtual "particles" around the ocean.

ARIANE interpolates the NEMO output to solve for particle translation through model grid cells and saves particle positions daily. The fact that ARIANE (and other Lagrangian analysis packages) make use of preexisting model output makes it a powerful tool to answer questions where an online model run with passive tracers would be prohibitively computationally expensive (Van Sebille et al., 2018). However, small-scale processes which are parameterized in the model, such as mixing and diffusion, cannot be directly assessed by Lagrangian analysis of advective pathways in a straightforward way (Wagner et al., 2019).

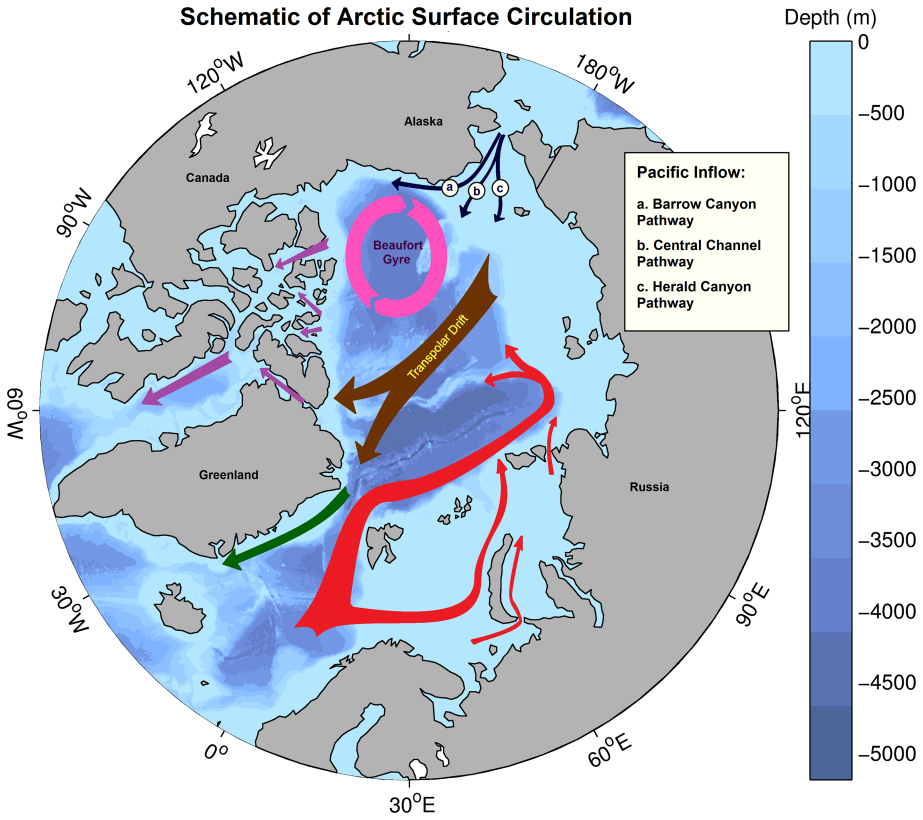

Figure 1. Schematic of large-scale Arctic Ocean circulation pathways. In dark blue, the three main Pacific inflow pathways are highlighted, via the Barrow canyon, Central Channel, and herald canyon. The anticyclonic Beaufort gyre is highlighted in pink. The transpolar drift, which brings water from Siberia to the Atlantic, is shown in brown. Water exits the Arctic via either the Fram Strait by following the East Greenland current, shown in green, or via the Canadian Arctic archipelago (CAA). Pathways through the archipelago are complex, and example pathways are highlighted with purple arrows. Finally, the red arrows show Atlantic water circulation pathways, entering via the eastern Fram Strait and Barents Sea opening, before following the Arctic circumpolar boundary current cyclonically along the Eurasian shelf break.

Lagrangian analysis has been widely used to investigate the Arctic Ocean in NEMO. Relevant to the research undertaken here, Pacific inflow pathways have been investigated using ARIANE in conjunction with an Arctic regional configuration of NEMO (Hu & Myers, 2013), and online passive tracer multimodel intercomparison experiments (Aksenov et al., 2016) have since supported these results. Outflow from the Arctic to the Atlantic Ocean (via Fram and Davis Straits) was investigated in a coarser ¼ resolution version of NEMO (Lique et al., 2010). Other questions, including the dynamics of the Beaufort Gyre (Kelly et al., 2019) and the fate of potential oil spills from Arctic shipping (Kelly et al., 2018), have used ARIANE alongside the same configuration of NEMO employed in this paper.

2.2. Experiment Design

First, the Eulerian changes in Arctic surface currents were investigated. We compared the mean current speeds for each decade (1970s–2000s) to the overall mean for that period. The lack of coherence in the decadal anomalies, with some regions accelerating and others slowing down (see Figure 2a), motivated a Lagrangian experiment to investigate changing connectivity between the North Pacific and Atlantic Oceans.

For each Lagrangian experiment, 1,000 particles were initialized, uniformly distributed across the Bering Strait. These particles were then tracked for 10 years, with positions recorded daily. “Releases” of particles took place every month between 1970 and 2003, with the same initial 1,000-particle grid used for each experiment. The initial release of each year was performed on the 5 January, with subsequent releases taking place at 30-day intervals beyond that. Particles were initialized in the surface layer of the ocean and then advected via ocean currents (not sea ice velocities) in three dimensions. No diffusion was manually added to the

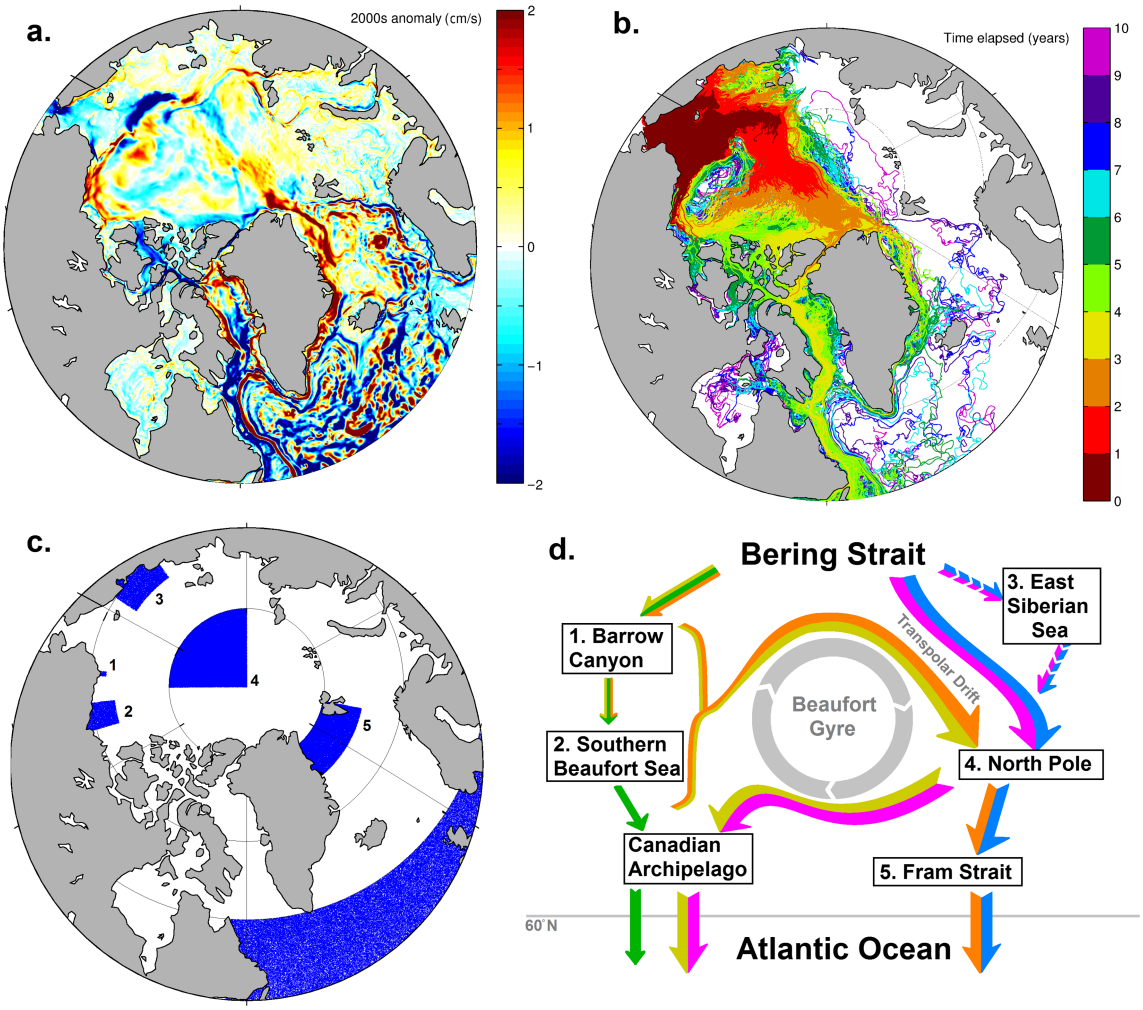

Figure 2. (a) The anomaly in NEMO-modeled Eulerian surface currents between 2000 and 2009, relative to the 1970–2009 mean. No uniform pattern is apparent, with some regions accelerating and others decelerating, necessitating a Lagrangian approach to investigate changing Pacific to Atlantic connectivity. (b) Example of output from Lagrangian experiments, showing the trajectories of all 1000 particles released in September 1980 (arbitrary choice of year/month). Color of trajectories denotes their age. (c) Map showing the location of the "traps" used to classify trajectories from the Lagrangian experiments. 1 = Barrow canyon, 2 = southern Beaufort Sea, 3 = east Siberian Sea, 4 = north pole, and 5 = Fram Strait. Also shown is the 60°N trap in the Atlantic Ocean, considered the end of each trajectory. Traps 1–3 only recorded particles which passed through in the first 2 years of the experiment. Trajectories which reach the Atlantic Ocean trap without passing through the Fram Strait are assumed to have passed through the CAA instead. (d) Simplified schematic showing the five main advective pathways identified using the traps in (c). See Table 1 for a more detailed explanation of how these pathways were defined.

advective signal read-in from the NEMO, in order to maximize the generality of our experiments. For example, some species are able to control their buoyancy in order to remain in the upper mixed layer. In these cases, manually adding diffusion (e.g., via a random walk) would not be desirable given the biological context of these experiments, and so we only consider the impact of advection in order to keep the experiments as generic as possible.

After their release in the Bering Strait, the advective pathways followed by each of particles were characterized by using various "traps" to define the route taken to reach the Atlantic Ocean. The definition of distinct pathways is discussed in more detail in section 3.1. Each "trap" is simply a region on the globe, and if a particle spends a time step within its defined latitude and longitude limits, it is recorded as having passed through said trap. By comparing which traps each particle does or does not pass through, it is possible to define distinct advective pathways. Grouping these pathways into meaningful routes allows us to compare how the connectivity between the Pacific and Atlantic has changed over the duration of the experiment, by considering how the number of particles following each defined route varies with year and season of release.

This trap-based approach has intrinsic limitations. As particle locations are recorded at discrete points rather than continuously, it is in principle possible for a particle to "skip over" a trap that, physically, a water parcel would have passed through in reality. This can be accounted for by using large traps, at the cost of having rather broadly defined pathways. Where smaller traps are necessary to be physically meaningful (e.g., the Barrow Canyon trap in section 3.1), the impact of overshooting can be mitigated by including an extra trap downstream to tag any particles that would otherwise have been missed.

As well as being interested in the routes taken to reach the Atlantic, we also need to consider the time taken. To do this, we define a single end trap, taken to be everything south of 60°N in the Atlantic Ocean. Other definitions of when a particle has reached the Atlantic are possible (e.g. one could consider anything south of the Fram Strait), but this limit was chosen to approximately coincide with the region where *N. seminae* was first recorded in 1999 (Reid et al., 2007), thus making it a logical end goal when considering Atlantic to Pacific connectivity. When considering timescales, we make a point to consider the trajectories with the shortest connectivity timescales. The reason for this is that accelerated Pacific to Atlantic connectivity has been hypothesized to be a cause for Pacific species reaching the Arctic. If minimizing the total time spent in harsh (for subpolar species) Arctic conditions is the limiting factor for a successful trans-Arctic crossing, focusing on the connectivity pathways with the shortest advective timescales makes sense.

3. Results

In order to address the first hypothesis identified in section 1, we begin by comparing Eulerian output from the NEMO model as a first attempt to address whether the surface currents in the Arctic Ocean have accelerated. To do this, we took the annual mean modeled surface currents from the period studied in these experiments and compared how each decade varied compared to the overall mean.

The 2000s anomaly is presented in Figure 2a as an illustrative example. It is apparent from this that there is no spatially coherent pattern to the changes in sea surface velocities: Some regions accelerate, others decelerate, and some currents shift their position. A similar lack of coherence was found for the 1970s, 1980s, and 1990s (not shown). This, coupled with the multiyear timescales required for trans-Arctic crossings, makes addressing either Hypothesis 1 or Hypothesis 2 from an exclusively Eulerian viewpoint inconclusive.

This necessitates investigating the problem from a Lagrangian viewpoint. As described in section 2, we do this by releasing virtual "particles" into the NEMO model in the Bering Strait and tracking their progress over 10 years. One thousand particles were released every month between January 1970 and December 2002. As an illustrative example of the output produced by these experiments, all trajectories from the September 1980 release (arbitrary choice of experiment) are shown in Figure 2b.

The trajectories in Figure 2b are colored to highlight the advective pathways with the shortest connectivity timescales. This is useful for giving a first-order estimate of the fastest advective timescales between the Bering Strait and the Atlantic Ocean (approximately 4 years), but at the price of masking much more of the detail. In order to extract more meaningful information from these trajectories, it is helpful to classify them based on shared characteristics. We do this by introducing "traps" to identify which particles pass through given regions (and those which do not).

3.1. Characterizing Different Connectivity Pathways

From what is already known about the Arctic Ocean circulation, as well as trajectory maps such as Figure 2b, the following traps were decided on to elucidate distinct pathways:

Trap 1: Barrow Canyon: South of 72°N, between 155°W and 157°W;

Trap 2: Southern Beaufort Sea: South of 73°N, between 135°W and 145°W;

Trap 3: East Siberian Sea: South of 73°N, between 155°E and 175°E;

Trap 4: North Pole: North of 80°N, between 120°E and 150°W;

Trap 5: Fram Strait: Between 75°N and 80°N, between 25°W and 20°E;

and finally, an "end" trap south of 60°N in the Atlantic Ocean (between 70°W and 20°E).

These traps are shown geographically in Figure 2c. The logic behind this choice of traps is as follows:

Traps 1 and 2 were chosen to sample the Alaskan Coastal Current, which flows through the Barrow Canyon into the Beaufort Sea. Trap 1 records particles which spend at least one time step in this part of the Barrow Canyon, but, as it is a relatively small trap, it is possible for some trajectories to overshoot it. The larger Trap 2 is therefore included to catch the minority of particles which follow the same pathway but would otherwise have been missed. In both cases, a particle is only tagged by these traps if it passes through them within the first 2 years of its trajectory, in order to avoid false positives from particles recirculated by the Beaufort Gyre.

Trap 3 was chosen because, as can be seen in Figure 2b, some trajectories begin by flowing from the Chukchi Sea into the East Siberian Sea. This trap quantifies those, although they are later grouped with other pathways (as suggested by Figure 2d). As with Traps 1 and 2, this trap is only triggered in the first 2 years of particles' trajectories.

Trap 4 was designed to sample the Transpolar Drift Stream. Necessarily a large trap, due to the shifting position of the Transpolar Drift due with the shift of the Beaufort Gyre, the vast majority of trajectories are tagged by this trap. Unlike the previous three, this trap can be triggered at any time.

Trap 5 defines the route trajectories take out of the Arctic Ocean. Only two options are available: Fram Strait or CAA. Any trajectory that exits the Arctic without triggering the Fram Strait trap is assumed to have come through the CAA instead (this assumption is valid; see Figure 3). In principle, one could further investigate the myriad of possible pathways through the archipelago, but we chose to simplify the problem by considering it a singular route. An alternative method could use a single trap for the whole CAA, but owing to the complex flow in this region with some particles recirculated in and out of the periphery of the archipelago, it is simpler (and avoids false positives) to classify CAA trajectories based on their avoidance of the Fram Strait.

Finally, the Atlantic Trap was chosen to be at 60°N because this marks a consistent end point, regardless of which side of Greenland trajectories flow. It is also an interesting choice from a biological perspective, as it also corresponds approximately to the region where nonnative phytoplankton were found to be blooming in (Reid et al., 2007).

Using these traps, we were able to identify distinct advective pathways and group them into five main routes, as illustrated in Figure 2d. The grouping was done after identifying every possible combination of traps and counting the fraction of trajectories which triggered each set. Each unique combination of traps was termed a "pathway." Pathways which were followed by at less than 0.1% of trajectories (i.e., an average of less than one trajectory per experiment) were considered negligible.

Of the nonnegligible pathways, similar pathways were identified and grouped together into "routes" (pathways with <0.1% of trajectories were also included in the groupings if sufficiently similar). Five main routes were identified, as shown by the simplified schematic in Figure 2d. These are as follows:

- The "pink route," which follows the transpolar drift and exits the Arctic Ocean via the CAA. Pathways 2 and 6.
- The "blue route," which follows the transpolar drift but leaves the Arctic via the Fram Strait (with both this and the pink route, trajectories are considered part of the same route regardless of whether or not they enter the East Siberian Sea). Pathways 3 and 7.
- The "yellow route," which enters the Arctic via Barrow Canyon, changes direction, and then joins the pink route to follow the Transpolar Drift and exit via the CAA. Pathways 10, 18, and 26.
- The "orange route," which begins like the yellow route (Barrow Canyon, then reversing to join the Transpolar Drift) but leaves through the Fram Strait as with the blue route. Pathways 11, 29, and 27.
- The "green route"—a markedly different pathway followed by a minority of particles. The green route enters the Beaufort Sea via Barrow canyon, then flows directly to the CAA. It is the only major pathway which does not interact with the Transpolar Drift Stream. Pathways 8* and 24*. In addition to the traps described above, this group was further filtered to remove false-positive trajectories which trigger the trap after becoming entrained in the Beaufort Gyre. This is done by removing trajectories north of 75°N in the Beaufort Gyre region.

Additionally, "other" trajectories which do not fit well into these definitions were identified. The majority of these are attributed to pathway 16, which appears to be something between the yellow route and the

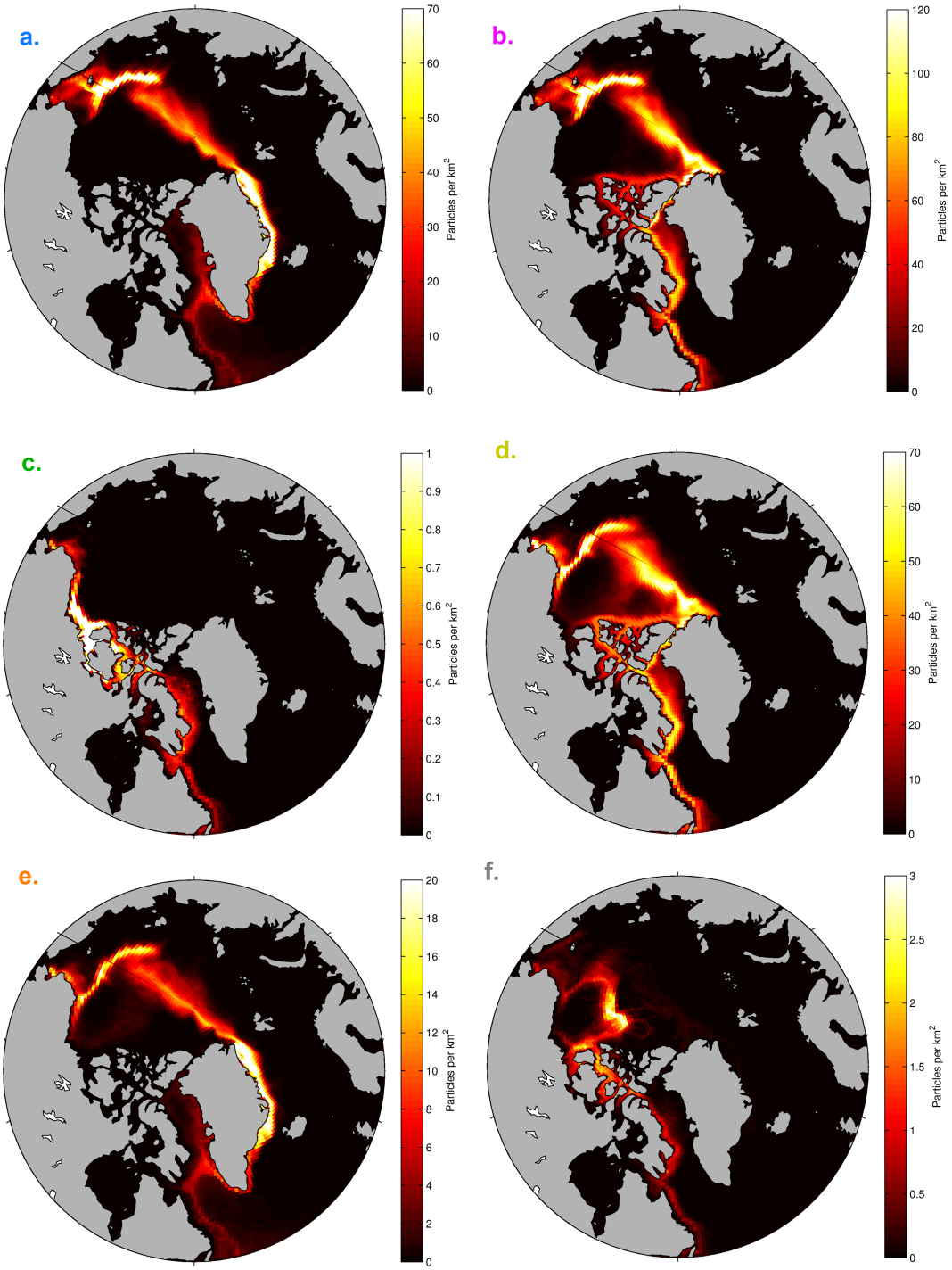

Figure 3. A more detailed illustration of the advective pathways identified in Figure 2d. In each subplot, trajectory density (particles/km^2) is shown. Note the different scales in each panel. From each route, every particle's position at each time step was binned into a 0.5° (lat) × 1° (lon) grid, then weighted by cell area to produce these density maps. (a) "blue route" from Figure 2d, comprised of trajectories avoiding Barrow canyon and joining the transpolar drift before exiting the Arctic via the Fram Strait. (b) "pink route" from Figure 2d. Initially the same as the blue route, this pathway branches off to exit the Arctic via the Canadian Arctic archipelago (CAA) instead of the Fram Strait. (c) "green route" from Figure 2d, comprised of trajectories which reach the Beaufort Sea via Barrow canyon and then flow directly through the CAA to the Atlantic. (d) "yellow route" from Figure 2d, flows through the Barrow canyon as in the green route before changing direction to join the transpolar drift and then leave the Arctic via the CAA. (e) "Orange route" from Figure 2d. Initially the same as the yellow route, but branches off to exit the Arctic via the Fram Strait. (f) Trajectories not assigned to any of the previous five advective pathways.

Table 1
Classification of Distinct Pathways Using the "Traps" Identified in Figure 2c

Pathway number	1. Barrow canyon	2. Southern Beaufort Sea	3. East Siberian Sea	4. North pole	5. Fram Strait	Percent of all trajectories
0						<0.1
1					✓	0
2				✓		40.1
3				✓	✓	18.0
4			✓			0
5			✓		✓	0
6			✓	✓		4.3
7			✓	✓	✓	3.2
8*		✓				<0.1
9		✓			✓	0
10		✓		✓		<0.1
11		✓		✓	✓	<0.1
12		✓	✓			0
13		✓	✓		✓	0
14		✓	✓	✓		0
15		✓	✓	✓	✓	0
16	✓					0.3
17	✓				✓	<0.1
18	✓			✓		25.2
19	✓			✓	✓	4.8
20	✓		✓			0
21	✓		✓		✓	0
22	✓		✓	✓		<0.1
23	✓		✓	✓	✓	<0.1
24*	✓	✓				0.2
25	✓	✓			✓	0
26	✓	✓		✓		3.1
27	✓	✓		✓	✓	0.7
28	✓	✓	✓			<0.1
29	✓	✓	✓		✓	0
30	✓	✓	✓	✓		<0.1
31	✓	✓	✓	✓	✓	<0.1

Note. Only trajectories which reached the final Atlantic Ocean (60°N) trap are considered. The final column shows the percentage of trajectories which reached the Atlantic Ocean that followed a given pathway. Minor pathways followed by <0.1% of trajectories were initially deemed to be negligible. Other pathways were grouped, along with similar pathways (including minor pathways), into five "routes" (see Figures 2d and 4) denoted by the color which their row is highlighted. Pathways 8* and 24* were further processed to exclude particles entrained into the Beaufort Gyre by removing trajectories which passed north of 75°N in the Beaufort Gyre region (in both cases, the trajectories removed accounted for <0.1% of all trajectories which reached the Atlantic). Pathway 16 was nonnegligible (0.3% of trajectories) but does not fit well into our classification system and is instead grouped with "others."

periphery of the Beaufort Gyre (see Figure 3f). The full list of pathways, the total number of particles (that reach the Atlantic Ocean) following them, and their groupings are presented in Table 1:

Having grouped our trajectories into five main routes, it is now possible to compare how they differ spatially and vary temporally. Maps showing trajectory density for each of the five routes, as well as the "other" group, are presented in Figure 3.

Figures 3a and 3b (pink and blue routes) show significant Pacific inflow through Herald Canyon (see north-south-oriented white region on the American side of Wrangel Island), which is absent in Figures 3c–3f, despite Herald Canyon not being explicitly defined with a trap.

Figures 3c–3e all show a clear pattern of inflow dominated by Barrow Canyon, demonstrating that the "trap" method used here works well. The return flow toward the Transpolar Drift is clearly present in Figures 3d and 3e, supporting the picture in the simplified schematic in Figure 2d.

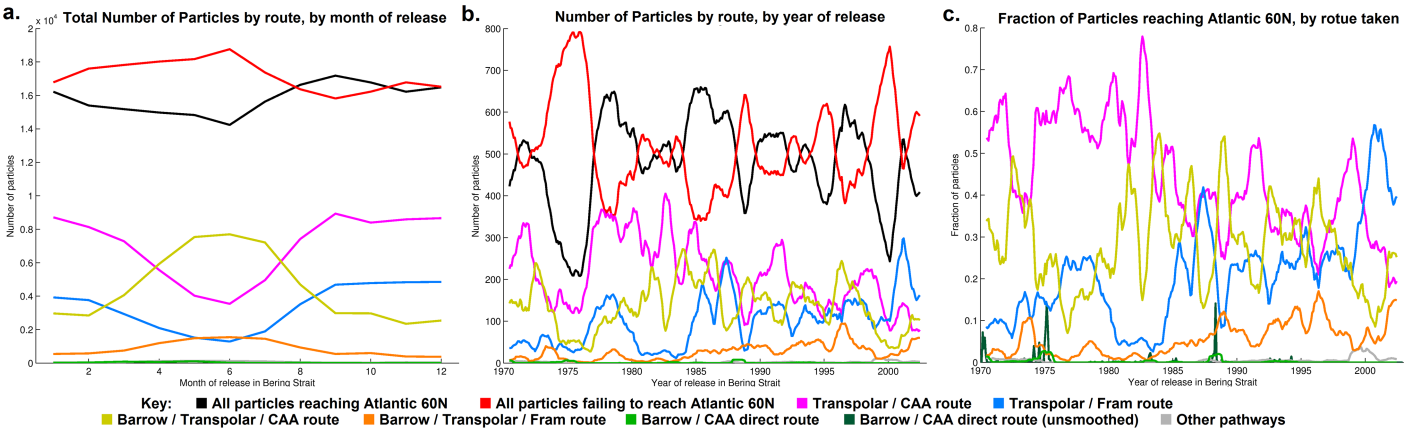

Figure 4. a) Comparison of the number of trajectories reaching (black) or failing to reach (red) 60N in the Atlantic Ocean within 10 years of being released in the Bering Strait. Other colors show how the routes taken vary by season – see key for explanation of each color. Trajectories passing (not passing) through the Barrow Canyon are more (less) frequent in spring/summer releases than in autumn/winter. b) Comparison of the number of trajectories reaching (black) or not reaching (red) 60N in the Atlantic Ocean, and following each route (all other colors) by time of release, in all cases with the seasonal cycle in (a) removed by taking a running 12-month average. The (non-Barrow Canyon) transpolar drift to Canadian Arctic Archipelago (pink) route is the dominant pathway for the majority of the experiment, before being usurped by the (non- Barrow Canyon) transpolar drift to Fram Strait route towards the end of the study period. c) Comparison of the trajectories which reach 60N in the Atlantic Ocean, showing the fraction of 'successful' trajectories which take each path way. As in (b), a running 12-month average is used to remove the seasonal cycle, with the exception of the dark green line, to demonstrate that although typically either unavailable or negligible, the green pathway can represent a significant number of trajectories when available.

Notably, the pathway through the Canadian Archipelago is visibly different in Figure 3e compared to the other main CAA pathways (Figures 3b and 3d). Figure 4f demonstrates that the "other" routes appear to be something between the green and yellow routes identified from our traps—it flows around the northern periphery of the Beaufort Gyre but passes through the Canadian Archipelago via a path more similar to the green than yellow/pink routes.

3.2. Variability of Pacific-Atlantic Routes

Having identified the main advective pathways connecting the Bering Strait to the Atlantic Ocean and how they differ from each other, we now investigate how they vary with time. Initially, we simply consider how the number of particles successfully reaching the Atlantic Ocean changes. From Figures 4a and 4b (red and black lines), it is clear that the number of "successful" trajectories is sensitive to time of release but that the 10-year experiment duration is sufficient for approximately half (47.7%) of all trajectories to reach the Atlantic trap. The large number of particles remaining in the Arctic for the duration of the experiment should not be unexpected, in no small part due to those which become entrained into the Beaufort Gyre (e.g., Kelly et al., 2019). From Figure 4a, we can see that late summer releases typically had the greatest chance of reaching the Atlantic within 10 years. Figure 4b shows significant interannual variability in whether or not trajectories successfully reach the Atlantic Ocean.

Investigating the seasonal cycle (Figure 4a) further shows that there is a clear oscillation whereby the pink and yellow routes (both via Barrow Canyon) are favored in spring/summer, whereas the blue and pink routes (both via Herald Canyon) are favored in autumn/winter. This is in line with well-established seasonality in the Pacific inflow to the Arctic Ocean (Aksenov et al., 2016). Three main Pacific inflow pathways are known to exist: the Alaskan Coastal Current/Beaufort shelf break jet through Barrow Canyon, a pathway through the Herald Canyon, and a central channel via the Herald and Hana Shoals (Timmermans et al., 2014). The Beaufort shelf break jet, corresponding to the yellow, green, and orange pathways here, is known to peak in summer (Lin et al., 2016).

The sensitivity to time of release was similarly investigated by tracking the number of trajectories following each route based on when they were released. This is shown in Figure 4b, where the time series has been smoothed by applying a 12-month running average to remove the seasonal cycle evident in Figure 4a. Given the sizable variation in the number of particles reaching the Atlantic by year, it makes more sense to consider the relative number of trajectories following each route than the raw numbers shown in Figure 4b; the relative fraction of trajectories following each route is shown in Figure 4c.

Figure 4c yields several interesting results. The first thing that can be noted is that the pink (Herald Canyon–transpolar drift–CAA) route is the dominant advective pathway throughout the 1980s, before declining and eventually being replaced by the blue (Herald Canyon–transpolar drift–Fram Strait) route in the later years of the experiment. The yellow (Barrow Canyon–transpolar drift–CAA) route shows considerable interannual variability but no clear trend, and the orange (Barrow Canyon–transpolar drift–Fram Strait) route shows a small positive trend. In all cases, the trends have considerably more noise than the more significant trend evident in Figure 4a, and the statistical significance of these trends is impacted by the interannual variability in number of successful trajectories. Some real variability due to the Arctic Oscillation (AO) may be expected (Morison et al., 2012; Steele et al., 2004), but artifacts of model spin-up is another possible explanation discussed in section 4.

The green (Barrow Canyon–Beaufort Sea–CAA) route and "other" routes are largely negligible when considering the 12-monthly rolling average. However, using a rolling average masks the true importance of the intermittent green route. In Figure 4c, the unaveraged time series for the green route is shown in darker green. While still usually negligible, there are two major peaks—1975 and 1988—where the green route represents >10% of successful trajectories. Thus, we identify this as an intermittent yet significant advective pathway for Pacific to Atlantic connectivity. The importance of this route becomes apparent when considering advective timescales and is discussed more thoroughly in section 4.1.

3.3. Advective Timescales

We now move on to considering the differences in connectivity timescales between the Pacific-Atlantic connectivity pathways. As we are interested in ecological connectivity, for example, nonnative planktonic species being brought from the Pacific to the Atlantic, it is sensible to consider the fastest cross-Arctic transits. This is for two reasons: Each particle represents a large volume of water, potentially containing a large volume of biomass, so even one particle in our Lagrangian experiments could be sufficient to explain a phytoplankton bloom. Second, the Arctic is a harsh environment, so it stands to reason that minimizing the time spent in the Arctic corresponds to maximizing the survival chances of subpolar Pacific species.

In Figure 5a, we present the shortest advective timescale along each route from each release. This produces a noisy time series (which is smoothed in Figure 5b), but unlike in Figure 4, this cannot be attributed to a seasonal cycle: As Figure 5c shows, aside from a small trend whereby summer releases take less time for the yellow and orange routes (both via Barrow Canyon), there is no seasonal trend for the also noisy blue and pink routes.

Nevertheless, the same 12-monthly running average was applied to smooth the data and attempt to elucidate a trend. No clear long-term trend showing a shortening/lengthening on the typical advective timescales was found in this experiment; however, it can be noted that both Fram Strait routes (blue and orange) took up to 2 years longer than was typical for the other routes during the first half of the 1980s, during which time the number of particles following the blue route also dropped (Figures 4b and 4c). Aside from this, the advective timescales associated with four most important (by number of trajectories) pathways largely varied in phase with each other. We can also note that the "other" group of pathways consistently has a much longer associated timescale than the other routes, justifying our decision to neglect them from the main routes.

Taking a running average of the green route makes little sense given the intermittency of this route (see faint green line in Figure 5b). For this reason, the connectivity timescales associated with this route are plotted as individual dots as and when the route exists. It is interesting to note that, in the releases identified in Figure 4 c as having an anomalously large fraction of particles following this pathway, the green route takes approximately 1 year less to reach the Atlantic than any of the other routes. As well as the 1975 and 1988 peaks identified in Figure 4, this pathway provides anomalously rapid transport to the Atlantic for other releases in the early 1980s and early 1990s. We identify this not just as a markedly different advective pathway from the more common transpolar routes but also as a potential shortcut.

The distribution of connectivity timescales (binned at 1/12 yearly frequency) is presented in Figure 5d. This shows skewed distribution, with a relatively sharp cutoff on the short timescale side and a much longer tail for long connectivity timescales. In order to test how well our 1,000 particles-per-release experiments capture extreme values at the short-timescale end of the distribution, we performed a subsampling experiment. This was done by randomly sampling (without replacement) 1%, 2%, ... , 98%, 99% of connectivity timescales and

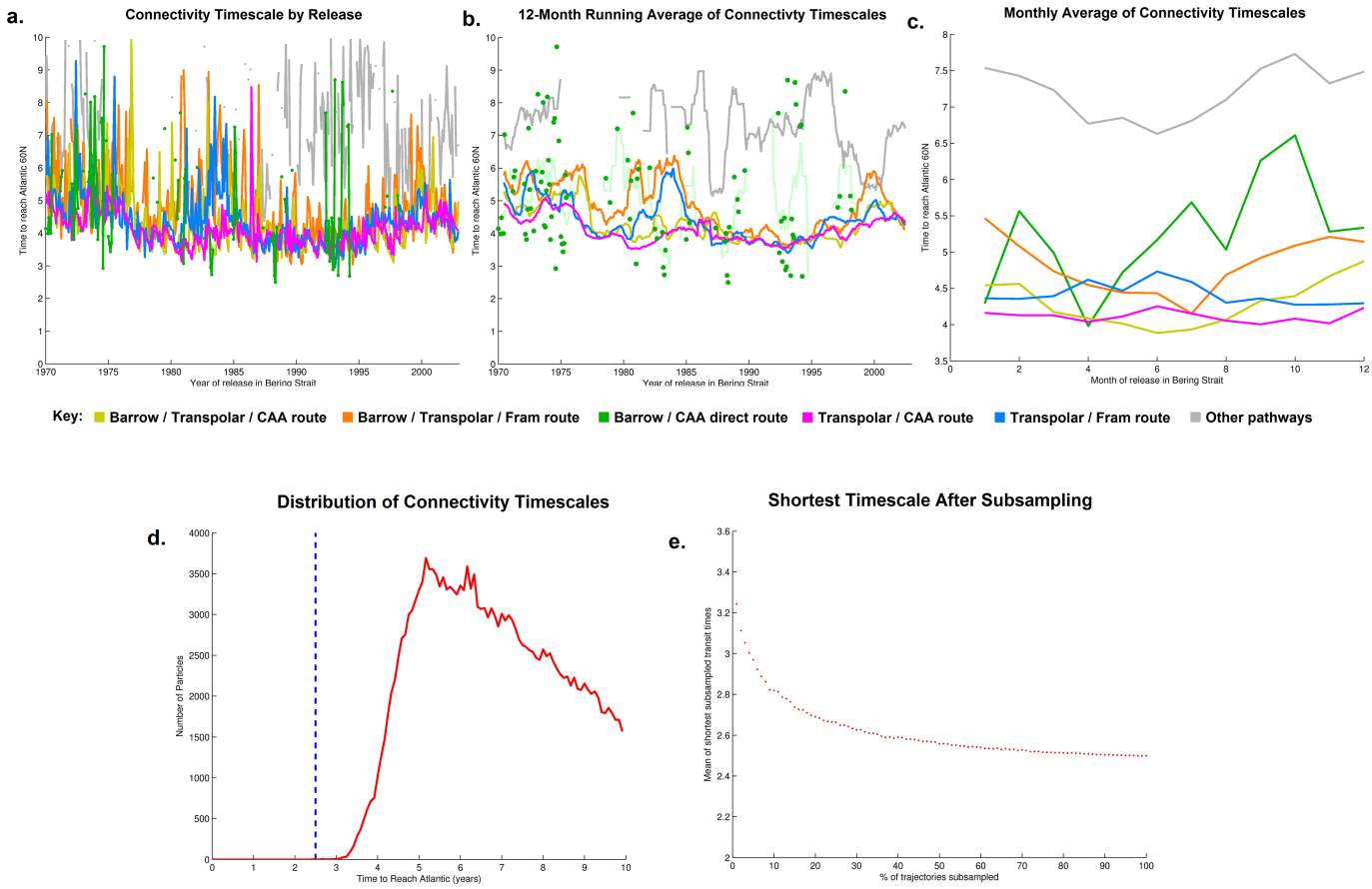

Figure 5. (a) Comparison of how connectivity timescale, defined to be the time taken by the first trajectory to reach 60°N in the Atlantic Ocean, varies with time of release for each of the routes identified in Figure 2d. No clear trend is evident, and variability between releases is considerable in all routes. (b) Comparison of connectivity timescales, this time smoothed with 12-montly rolling averages. Years on which no trajectories followed a route are ignored. Due to the green route only being occasionally available, the timescale for each release is plotted as a dot rather than the running average. (c) Monthly averages of connectivity timescales for each route. No trend is apparent for the pink, blue, or green routes; however, the orange and yellow routes have shorter connectivity timescales in summer than in winter. (d) Distribution of all connectivity timescales, binned at 1/12 yearly intervals. Dashed blue line shows the absolute shortest timescale (2.50 years) recorded. (e) Mean of absolute shortest remaining connectivity timescale, after random subsampling (without replacement) at the rate shown by the *x*-axis 1000 times.

comparing the minimum remaining timescale in each case. This subsampling was repeated 1,000 times, with the mean shortest remaining connectivity timescale recorded for each subsampling rate. The result of this is shown in Figure 5e. The trend becomes asymptotic as the subsampling rate tends to 100%, and even reducing the number of particles by a factor of 10 only increases the minimum timescale by ~3 months. This suggests that the shortest connectivity timescales recorded in our experiments are a good approximation of the true minima that would be recorded with an arbitrarily large number of trajectories.

4. Discussion

4.1. Variability and Trends in Advective Pathways

The four main advective pathways (blue, pink, yellow, and orange) described in section 3.1 show significant temporal variability, both seasonally and interannually. The seasonal variability, seen in Figure 4a, shows a clear split between Pacific inflow to the Arctic via Barrow Canyon (yellow and orange) and other pathways (blue and pink), with the Barrow Canyon pathways favored by particles released in the Bering Strait during spring/summer and the other pathways favored by autumn/winter releases.

This is in agreement with previous research into Pacific Water pathways in the Arctic Ocean (Aksenov et al., 2016; Timmermans et al., 2014), which note three main Pacific Water pathways across the Chukchi Sea: a

branch through Barrow Canyon (corresponding to the orange, yellow, and green routes in our experiment), a branch through Herald Canyon, and flow between the two over the central shelf. We group the latter two pathways together, both of which contribute to our blue and pink routes here.

The yellow, orange, and green routes which flow through Barrow Canyon are attributed to the Beaufort Sea shelf break jet (von Appen & Pickart, 2012). The relative increase/decrease in number of trajectories following these pathways is in agreement with the seasonal cycle of cyclonic (winter) and anticyclonic (summer) atmospheric wind forcing (Proshutinsky et al., 2009), which we would expect to drive an Ekman transport conveying trajectories either toward (summer) or away from (winter) the shelf break jet.

As von Appen and Pickart (2012) note, the winter configuration of the shelf break jet can extend over a sufficient distance that it should be able to reach the Canadian Archipelago. This is in agreement with the pathway followed by the green route in our Lagrangian experiments. However, the majority of Pacific Water transported to the Atlantic is known to follow the transpolar drift (Nguyen et al., 2011). Our results also support this, with the "green route" identified here being dwarfed by the four other routes (all of which are characterized by following the transpolar drift).

The interannual variability of advective pathways was also investigated. Significant interannual variability, but no clear trend, was found between the relative importance of the Barrow Canyon (orange, yellow, and green) and non-Barrow Canyon routes. A trend was apparent in the exit points to the Atlantic Ocean, however. For particles released in the Bering Strait between 1980 and 2003, there was a relative increase in pathways exiting via the Fram Strait. Observations show that the Pacific connectivity to the Canadian Archipelago and/or Fram Strait is linked to the AO regime (Morison et al., 2012; Steele et al., 2004); however, due to the start of the experiment being relatively close to the beginning of the model run, the effect of model drift due to the spin up period cannot be discounted as another possible influence on these trends. Barotropic circulation spin-up typically takes few months, and baroclinic circulation trend is 2% per year after ~20 years (Aksenov et al., 2016; Wang et al., 2016); however, this is difficult to disentangle with varying forcing.

4.2. Causes of Intermittent "Green Route"

As identified in section 3.3, the "green route" can have an anomalously rapid connectivity timescale, in some cases over a year shorter than all other pathways. However, as previously noted in section 3.2, the availability of this pathway is intermittent. From Figure 4c, the two clearest examples of this route existing as a major pathway occur in 1975 and 1988.

In order to investigate potential causes for the pulse-like nature of this pathway, we compare two indices that describe the large-scale behavior of the Arctic Ocean: the AO and the Arctic Ocean Oscillation (AOO). Both of these metrics describe the cyclonicity (or anticyclonicity) of the Arctic: In the case of the AO, the index describes the relative strength of the anticyclonicity of the large-scale atmospheric forcing driving the ocean (Thompson & Wallace, 1998), with negative indices corresponding to stronger anticyclonic winds. The AOO is an index derived from a two-level model to describe the barotropic component of the ocean's response to atmospheric forcing: The sign and magnitude of the AOO are calculated as the gradient of sea surface height between the center and periphery of closed circulation in the Arctic (Proshutinsky & Johnson, 1997).

The signs of the two indices are essentially flipped, with positive AOO corresponding to an anticyclonic response from the Arctic Ocean and negative indices associated with a more cyclonic ocean (Proshutinsky et al., 2015; Proshutinsky & Johnson, 1997). These indices are presented in Figure 6a.

Figure 6a shows that describing the large-scale cyclonicity/anticyclonicity of the Arctic is not trivial, and the two indices do not always have opposite signs to each other. However, 1989—an anomalously cyclonic year—is clearly picked out by both measures. As well as showing the AO and AOO indices, Figure 6a highlights the two releases (March 1975 and May 1988) which had the greatest fraction of trajectories following the "green route" pathway that avoids the transpolar drift (see Figure 3c). Note that it is the initial time of release that is highlighted by the vertical lines in Figure 6a—even the trajectories with the shortest connectivity timescales take at least 2–3 years to reach the Atlantic, so trajectories are affected by forcing (at least) 2–3 years after the green lines indicates.

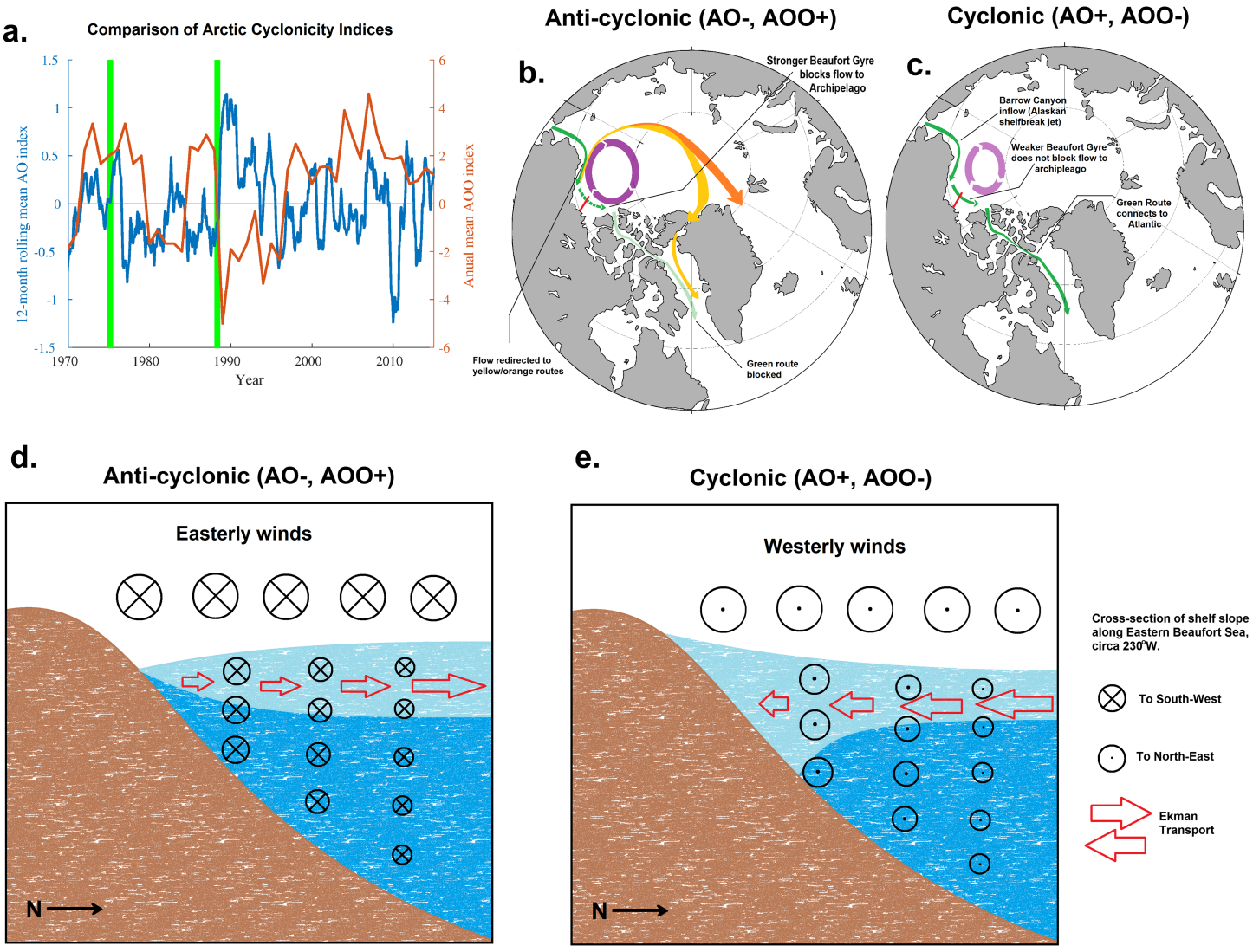

Figure 6. : (a) Comparison of the 12-monthly rolling mean Arctic oscillation (AO, blue) index taken from the NOAA, and the annual Arctic Ocean oscillation (AOO, orange) index over the period 1970–2015. Vertical green lines show the two release times that were associated with the largest fraction of trajectories following the "green route" (see figure 4c). (b) Simplified circulation schematic showing the anticyclonic regime in which the green route is blocked and diverted to yellow/orange routes. (c) Simplified circulation schematic showing the more cyclonic regime in which the green route is permitted. (d) Idealized cross section along red line in Figures 6b and 6c, under the anticyclonic regime. Easterly winds are favored, driving an Ekman transport away from the shore. By continuity, this induces a sea surface slope downwards toward the coast, which supports a barotropic geostrophic flow toward the west (stronger closer to the coast), which blocks the green route as in Figure 6b. (e) Idealized cross section along the same line, but in the cyclonic case that favors the green route in Figure 6c. Cyclonic regime favors westerly winds, which drives Ekman transport to the coast. By continuity, this induces a sea surface gradient up toward the shore, which in turn supports a geostrophic barotropic flow toward the Canadian archipelago.

A comparison of the circulation with the green route open/closed is presented in Figures 6b and 6c. The May 1988 release stands out as special because it has the single largest number of particles following the green route from any release in these experiments. The 1975 peak in Figure 4c is in part due to the relatively small number of particles reaching the Atlantic at all from that release, whereas the 1989 peak comes from a year with a greater fraction of "successful" trajectories.

It is also interesting to note that, shortly after these particles were released, the Arctic Ocean switched from anticyclonic to anomalously cyclonic—as highlighted in both the maxima in AO and minima in AOO indices in 1989. This also occurs in the AO index (though not the AOO) with the 1975 release.

We suggest that this increased cyclonicity is a driver for the "green route" Pacific to Atlantic connectivity pathway. The mechanism behind this is as follows: Cyclonic atmospheric forcing drives stronger westerly

winds along the Beaufort Sea shelf break, which causes an Ekman transport toward the coastline, causing downwelling at the coast. By continuity, this induces a slope in sea surface height, with a downward gradient away from the shore. This sea surface gradient in turn drives a barotropic current toward the Canadian Archipelago, consistent with the "green route" identified in Figure 3c. A simplified two-layer schematic of this is presented in Figure 6e.

Conversely, in the anticyclonic case, upwelling-favorable easterly winds (Brugler et al., 2014; Pickart et al., 2009) drive a barotropic current away from the Canadian Archipelago that serves to block the green route. The mechanism for this is the opposite of that in Figure 6e, as this time easterly winds create a downward sea surface gradient toward the coast, which induces the blocking current and prevents the green route from connecting to the Canadian Archipelago. This is presented schematically in Figure 6d.

Observational data, based on mooring arrays in the Beaufort Sea, support this idea. In January 2005, pulse-like enhancements of the Beaufort Sea shelf break current were recorded at a mooring in the southeast of the Beaufort Sea (Barber et al., 2015). This mooring (CA13) is located downstream of where trajectories following the "orange" and "yellow" routes diverge from the "green route" in Figure 3. Dmitrenko et al. (2016) investigated these pulse-like enhancements and found that they were associated with cyclones to the north of the shelf slope causing an Ekman transport toward the coast, creating a cross-slope pressure gradient in turn driving the eastward geostrophic current. Two modes of the shelf break current were identified, with downwelling-favorable winds driving a current along the Beaufort shelf toward the Canadian Archipelago, whereas upwelling-favorable winds drive an oppositely directed current to the west (Dmitrenko et al., 2018), which is in agreement with the mechanism described here. In a modeling study, Hu and Myers (2013) compared two routes ("Alaskan" and "Transpolar") linking the Pacific Ocean to the Canadian Archipelago and found connectivity timescales comparable to those presented here. They also noted wind-driven freshwater storage in the Beaufort Gyre as a driving mechanism of increased geostrophic transport along the Alaskan route during the model spin up period (Hu & Myers, 2013).

We propose that cyclonic wind-driven current events are responsible for providing the link between the well-established Alaskan shelf break current and the CAA. The intermittent, pulse-like nature of the geostrophic current observed by moorings (Barber et al., 2015; Dmitrenko et al., 2016) supports the pulse-like nature of the "green" Pacific to Atlantic connectivity pathway highlighted here.

4.3. Ecological Context

The most rapid advective pathways found in these experiments suggest that at least 2 years is required for a successful transit from Pacific to Atlantic via the Arctic Ocean and that the advective pathway permitting this was only sporadically open. Of the more typical advective pathways, the shortest possible connectivity timescales were 3–4 years, with a slight decrease in timescales occurring between 1970 and the mid-1990s.

As discussed in section 1.1, the key limiting factor between circulation connectivity is not just whether or not species from the Pacific could potentially reach the Atlantic, but whether or not they could make it there alive. For species with a pelagic larval stage, the PLD is another limiting factor that dictates whether passive circulation connectivity is sufficiently fast to permit ecological connectivity between two regions (Cowen et al., 2006; Selkoe & Toonen, 2011).

As these limiting timescales vary significantly between species (Bradford et al., 2015; van Herwerden et al., 2006), it is beyond the scope of this research to address whether or not the connectivity changes described in section 3 would constitute a tipping point for any particular species. However, with even the shortest Pacific to Atlantic connectivity timescales being greater than 2 years, our results suggest that the tipping point for any species requiring a single-summer transit to avoid Arctic winters is highly improbable. The >2-year connectivity timescales found here are beyond the PLD of rock lobsters at 18 months (Bradford et al., 2015) or even California morays at ~2 years (Higgins et al., 2017) but does not necessarily preclude a stepping-stone style transit with species reproducing along the journey (Selkoe & Toonen, 2011). Planktonic species, such as the diatom *N. seminae* which inspired this study (Reid et al., 2007), are not limited by PLD, and so >2-year transits cannot automatically be ruled out on that basis. However, assessing whether or not a tipping point has been reached for any individual species requires knowledge of the species life cycle, what conditions it requires to survive, and whether or not it could

reproduce in transit. It might be expected that shorter connectivity timescales, such as those in the green route highlighted here, could be more favorable as they minimize time spent in harsh Arctic conditions, but analysis of individual species is required to fully answer these questions.

4.4. Limitations and Future Work

The research presented here used a 1/12° resolution ocean model. This was the highest resolution model available to us, and it is important to note that connectivity pathways described here—including the anomalously short-timescale route through the Canadian Archipelago—pass through narrow passageways that may not be sufficiently well resolved in coarser models. How trans-Arctic connectivity could change in future decades remains an open question, but future-projection ocean models are typically only available at lower spatial resolution than used here (Yool et al., 2015). High-resolution models are required to accurately assess Pacific to Atlantic connectivity.

Offline Lagrangian modeling has the advantage that, by utilizing existing model output, it allows experiments that would otherwise be prohibitively computationally expensive to run. The Lagrangian particles in these experiments were driven by presaved output from the NEMO ocean model, and this was saved as 5-day means. However, this coarse time resolution loses the variability and structure in advection in the sub-hourly time steps that the model was run with online. This averaging could potentially remove anomalously fast and anomalously slow but short-lived currents.

In the context of these experiments, where we are primarily interested in the most rapid connectivity pathways, this implies another limitation of our experiments: There is a chance that the averaging of NEMO output used to drive our Lagrangian experiments could lengthen the shortest connectivity timescales reported here, potentially causing a systematic underestimate of connectivity timescales. Further, more computationally intensive experiments either run with Lagrangian particles or online tracers would be necessary to fully answer this question.

We are further limited by the use of only one ocean model run with only one forcing set. Although NEMO has been extensively validated (Aksenov et al., 2016; Janout et al., 2015; Kelly et al., 2019; Luneva et al., 2015), an intercomparison project using an ensemble of models would increase the validity of this work.

5. Summary and Conclusions

Three hypotheses that could potentially explain increased ecological connectivity between the North Pacific and North Atlantic Oceans were identified. These were (1) acceleration of advective timescales connecting the Pacific and Atlantic; (2) a change in relative importance of existing advective pathways and/or appearance of new, more rapid pathways; and (3) changing conditions along the route.

The third hypothesis is beyond the scope of this paper and remains an interesting open question for future research to address. The first and second hypotheses were investigated using a Lagrangian particle-tracking experiment.

Five main advective pathways, including one pathway which was only sporadically available, were defined. All four of the main advective pathways showed significant interannual variability in advective timescales, with an overall decrease from 5–6 to 4 years between 1970 and 1995 and a slight increase in advective timescales in the period 1995 to 2003. Even the absolute shortest advective timescales were still multiyear, implying that any species making trans-Arctic migrations would necessarily have to be capable of surviving Arctic winters in order to colonize the North Atlantic.

Two main trends in the relative importance of these advective pathways were found. A seasonal trend, with pathways favoring the Barrow Canyon in summer and other inflow pathways in the winter, was found, in line with previous research onto Pacific water pathways in the Arctic Ocean (Aksenov et al., 2016). Moreover, an interannual trend was found, showing the Fram Strait increasing in importance as an outflow pathway for Pacific to Atlantic connectivity since 1980, especially post 1989, replacing the Canadian Archipelago as the dominant outlet at the end of the experiment. The influence of the AO on Pacific connectivity to the Fram Strait and/or Canadian Archipelago has been discussed by Steele et al. (2004) and is one potential explanation for this, but model spin-up effects may also be a contributing factor.

In addition to the four main advective pathways, a fifth sporadically available and markedly different connectivity pathway between the Pacific and Atlantic Oceans was identified. This pathway (referred to as the "green" route here) follows the Barrow Canyon inflow after entering the Arctic Ocean but, unlike the main pathways, avoids the transpolar drift. Instead, this route sticks to the North American coastline, before exiting the Arctic via Parry Channel in the Canadian Archipelago.

This route is special from an ecological context because it is anomalously rapid compared to the main Pacific to Atlantic pathways. It has connectivity timescales in some cases over 1 year more rapid than other routes starting in the Bering Strait at the same time and is the only route which allows for below 3-year connectivity timescales between the Pacific and North Atlantic. From a biological perspective, this is potentially important because ecological connectivity requires connectivity pathways with a short enough timescale for Pacific species to reach the Atlantic alive. A sporadically available advective pathway with a shorter than usual connectivity timescale provides such a potential ecological connectivity pathway. However, the timescale required for a successful transit is dependent on both the species in question and the conditions it experience along route. Further research is required to establish whether or not this pathway has played a role in previous ecological transits or if it could play a role in future transits.

Acknowledgments
The underpinning high-resolution NEMO simulation was performed using the ARCHER UK National Supercomputing Service (http://www.archer.ac.uk). Lagrangian analysis was carried out using computational tool ARIANE developed by B. Blanke and N. Grima, using the JASMIN data analysis environment (http://www.jasmin.ac.uk). The 5-day mean output from the ORCA0083-N006 run of NEMO that was used to for the Lagrangian experiments is available on JASMIN (http://www.jasmin.ac.uk), and the Lagrangian trajectories produced in these experiments are publicly available on Zenodo with DOIs 10.5281/zenodo.3612713 and 10.5281/zenodo.3613665. Arctic Ocean Oscillation (AOO) index available from Woods Hole Oceanographic Institution: https://www.whoi.edu/page.do?pid=66578. This work has been supported by the APEAR (NE/R012865/1), ARISE (NE/P006000/1), Arctic PRIZE (NE/P006078/1), and DIAPOD (NE/P006353/1) projects, as part of the Changing Arctic Ocean program, funded by the UKRI Natural Environment Research Council (NERC) and, for APEAR, jointly funded with the German Federal Ministry of Education and Research (BMBF). This work was further supported by NERC grant CLASS (NE/R015953/1) and the COMFORT project (EU H2020; project number 820989). Finally, we would like to thank Erik van Sebille and another anonymous reviewer for their insightful comments which strengthened this work.

References

Aksenov, Y., Ivanov, V. V., Nurser, A. J. G., Bacon, S., Polyakov, I. V., Coward, A. C., et al. (2011). The Arctic circumpolar boundary current. *Journal of Geophysical Research, Oceans*, *116*, C09017.

Aksenov, Y., Karcher, M., Proshutinsky, A., Gerdes, R., De Cuevas, B., Golubeva, E., et al. (2016). Arctic pathways of Pacific water: Arctic Ocean model intercomparison experiments. *Journal of Geophysical Research, Oceans*, *121*, 27–59.

Aksenov, Y., Popova, E. E., Yool, A., Nurser, A. J. G., Williams, T. D., Bertino, L., & Bergh, J. (2017). On the future navigability of Arctic Sea routes: High-resolution projections of the Arctic Ocean and sea ice. *Marine Policy*, *75*, 300–317.

Appen, W.-J. V., & Pickart, R. S. (2012). Two configurations of the western Arctic shelfbreak current in summer. *Journal of Physical Oceanography*, *42*, 329–351.

Armitage, T. W. K., Bacon, S., Ridout, A. L., Petty, A. A., Wolbach, S., & Tsamados, M. (2017). Arctic Ocean surface geostrophic circulation 2003–2014. *The Cryosphere*, *11*, 1767–1780.

Armitage, T. W. K., Bacon, S., Ridout, A. L., Thomas, S. F., Aksenov, Y., & Wingham, D. J. (2016). Arctic Sea surface height variability and change from satellite radar altimetry and GRACE, 2003–2014. *Journal of Geophysical Research, Oceans*, *121*, 4303–4322.

Arteaga, L., Pahlow, M., & Oschlies, A. (2014). Global patterns of phytoplankton nutrient and light colimitation inferred from an optimality-based model. *Global Biogeochemical Cycles*, *28*, 648–661.

Bach, L., Zbawicka, M., Strand, J., & Wenne, R. (2019). *Mytilus trossulus* in NW Greenland is genetically more similar to North Pacific than NW Atlantic populations of the species. *Marine Biodiversity*, *49*, 1053–1059.

Bacon, S., Marshall, A., Holliday, N. P., Aksenov, Y., & Dye, S. R. (2014). Seasonal variability of the East Greenland coastal current. *Journal of Geophysical Research, Oceans*, *119*, 3967–3987.

Barber, D. G., Hop, H., Mundy, C. J., Else, B., Dmitrenko, I. A., Tremblay, J.-E., et al. (2015). Selected physical, biological and biogeochemical implications of a rapidly changing Arctic marginal ice zone. *Progress in Oceanography*, *139*, 122–150.

Blanke, B., & Raynaud, S. (1997). Kinematics of the Pacific equatorial undercurrent: An Eulerian and Lagrangian approach from GCM results. *Journal of Physical Oceanography*, *27*, 1038–1053.

Bradford, R. W., Griffin, D., & Bruce, B. D. (2015). Estimating the duration of the pelagic phyllosoma phase of the southern rock lobster, *Jasus edwardsii* (Hutton). *Marine and Freshwater Research*, *66*, 213–219.

Brodeau, L., Barnier, B., Treguier, A.-M., Penduff, T., & Gulev, S. (2010). An ERA40-based atmospheric forcing for global ocean circulation models. *Ocean Modelling*, *31*, 88–104.

Brugler, E. T., Pickart, R. S., Moore, G. W. K., Roberts, S., Weingartner, T. J., & Statscewich, H. (2014). Seasonal to interannual variability of the Pacific water boundary current in the Beaufort Sea. *Progress in Oceanography*, *127*, 1–20.

Cowen, R. K., Paris, C. B., & Srinivasan, A. (2006). Scaling of connectivity in marine populations. *Science*, *311*, 522–527.

Cowen, R. K., & Sponaugle, S. (2009). Larval dispersal and marine population connectivity. *Annual Review of Marine Science*, *1*, 443–466.

Dmitrenko, I. A., Kirillov, S. A., Forest, A., Gratton, Y., Volkov, D. L., Williams, W. J., et al. (2016). Shelfbreak current over the Canadian Beaufort Sea continental slope: Wind-driven events in January 2005. *Journal of Geophysical Research, Oceans*, *121*, 2447–2468.

Dmitrenko, I. A., Kirillov, S. A., Myers, P. G., Forest, A., Tremblay, B., Lukovich, J. V., et al. (2018). *Wind-forced depth-dependent currents over the eastern Beaufort Sea continental slope: Implications for Pacific water transport. Elem Sci Anth*, 6.

Fichefet, T., & Maqueda, M. a. M. (1997). Sensitivity of a global sea ice model to the treatment of ice thermodynamics and dynamics. *Journal of Geophysical Research, Oceans*, *102*, 12,609–12,646.

Goosse, H., & Fichefet, T. (1999). Importance of ice-ocean interactions for the global ocean circulation: A model study. *Journal of Geophysical Research, Oceans*, *104*, 23,337–23,355.

Higgins, B. A., Pearson, D., & Mehta, R. S. (2017). El Niño episodes coincide with California moray *Gymnothorax mordax* settlement around Santa Catalina Island, California. *Journal of Fish Biology*, *90*, 1570–1583.

Hu, X., & Myers, P. G. (2013). A Lagrangian view of Pacific water inflow pathways in the Arctic Ocean during model spin-up. *Ocean Modelling*, *71*, 66–80.

Janout, M. A., Aksenov, Y., Hölemann, J. A., Rabe, B., Schauer, U., Polyakov, I. V., et al. (2015). Kara Sea freshwater transport through Vilkitsky Strait: Variability, forcing, and further pathways toward the western Arctic Ocean from a model and observations. *Journal of Geophysical Research, Oceans*, *120*, 4925–4944.

Jönsson, B. F., & Watson, J. R. (2016). The timescales of global surface-ocean connectivity. *Nature Communications*, *7*, 11,239.

Kelly, S., Popova, E., Aksenov, Y., Marsh, R., & Yool, A. (2018). Lagrangian modeling of Arctic Ocean circulation pathways: Impact of advection on spread of pollutants. *Journal of Geophysical Research, Oceans*, *123*, 2882–2902.

Kelly, S. J., Proshutinsky, A., Popova, E. K., Aksenov, Y. K., & Yool, A. (2019). On the Origin of Water Masses in the Beaufort Gyre. *Journal of Geophysical Research: Oceans*, *0*.
Lin, P., Pickart, R. S., Stafford, K. M., Moore, G. W. K., Torres, D. J., Bahr, F., & Hu, J. (2016). Seasonal variation of the Beaufort shelfbreak jet and its relationship to Arctic cetacean occurrence. *Journal of Geophysical Research, Oceans*, *121*, 8434–8454.
Lique, C., Treguier, A. M., Blanke, B., & Grima, N. (2010). On the origins of water masses exported along both sides of Greenland: A Lagrangian model analysis. *Journal of Geophysical Research, Oceans*, *115*, n/a–n/a.
Luneva, M. V., Aksenov, Y., Harle, J. D., & Holt, J. T. (2015). The effects of tides on the water mass mixing and sea ice in the Arctic Ocean. *Journal of Geophysical Research, Oceans*, *120*, 6669–6699.
Madec, G. (2014). "NEMO Ocean engine" (draft edition r5171) "NEMO Ocean engine" (draft edition r5171). *Note du Pôle de modélisation, Institut Pierre-Simon Laplace (IPSL), France*, *27*, 1288–1619.
Matul, A., Spielhagen, R. F., Kazarina, G., Kruglikova, S., Dmitrenko, O., & Mohan, R. (2018). Warm-water events in the eastern Fram Strait during the last 2000 years as revealed by different microfossil groups. *Polar Research*, *37*. 1540243
Mayorga-Adame, C. G., Batchelder, H. P., & Spitz, Y. H. (2017). Modeling larval connectivity of coral reef organisms in the Kenya-Tanzania region. *Frontiers in Marine Science*, *4*.
Miettinen, A., Koç, N., & Husum, K. (2013). Appearance of the Pacific diatom Neodenticula seminae in the northern Nordic seas—An indication of changes in Arctic Sea ice and ocean circulation. *Marine Micropaleontology*, *99*, 2–7.
Morison, J., Kwok, R., Peralta-Ferriz, C., Alkire, M., Rigor, I., Andersen, R., & Steele, M. (2012). Changing Arctic Ocean freshwater pathways. *Nature*, *481*, 66.
Nguyen, A. T., Menemenlis, D., & Kwok, R. (2011). *Arctic Ice-Ocean Simulation with Optimized Model Parameters: Approach and Assessment*, (p. 116). Journal of Geophysical Research: Oceans.
Nurser, A. J. G., & Bacon, S. (2014). The Rossby radius in the Arctic Ocean. *Ocean Science*, *10*, 967–975.
Østreng, W., Eger, K. M., Fløistad, B., Jøgensen-Dahl, A., Lothe, L., Mejlnder-Larsen, M., & Wergeland, T. (2013). *Shipping in Arctic Waters: A Comparison of the Northeast, Northwest and Trans Polar Passages*. Berlin, Heidelberg: Springer.
Overland, J. E., & Wang, M. (2013). When will the summer Arctic be nearly sea ice free? *Geophysical Research Letters*, *40*, 2097–2101.
Peralta-Ferriz, C., & Woodgate, R. A. (2015). Seasonal and interannual variability of pan-Arctic surface mixed layer properties from 1979 to 2012 from hydrographic data, and the dominance of stratification for multiyear mixed layer depth shoaling. *Progress in Oceanography*, *134*, 19–53.
Pickart, R. S., Moore, G. W. K., Torres, D. J., Fratantoni, P. S., Goldsmith, R. A., & Yang, J. (2009). *Upwelling on the Continental Slope of the Alaskan Beaufort Sea: Storms, Ice, and Oceanographic Response*, (p. 114). Journal of Geophysical Research: Oceans.
Popova, E., Vousden, D., Sauer, W. H. H., Mohammed, E. Y., Allain, V., Downey-Breedt, N., et al. (2019). Ecological connectivity between the areas beyond national jurisdiction and coastal waters: Safeguarding interests of coastal communities in developing countries. *Marine Policy*, *104*, 90–102.
Proshutinsky, A., Bourke, R. H., & Mclaughlin, F. A. (2002). The role of the Beaufort gyre in Arctic climate variability: Seasonal to decadal climate scales. *Geophysical Research Letters*, *29*. 15-1-15-4
Proshutinsky, A., Dukhovskoy, D., Timmermans, M.-L., Krishfield, R., & Bamber, J. L. (2015). *Arctic Circulation Regimes*, (p. 373). Philosophical Transactions of the Royal Society A: Mathematical, Physical and Engineering Sciences.
Proshutinsky, A., Krishfield, R., Timmermans, M.-L., Toole, J., Carmack, E., Mclaughlin, F., et al. (2009). *Beaufort Gyre Freshwater Reservoir: State and Variability from Observations*, (p. 114). Journal of Geophysical Research: Oceans.
Proshutinsky, A. Y., & Johnson, M. A. (1997). Two circulation regimes of the wind-driven Arctic Ocean. *Journal of Geophysical Research, Oceans*, *102*, 12,493–12,514.
Reid, P. C., Johns, D. G., Edwards, M., Starr, M., Poulin, M., & Snoeijs, P. (2007). A biological consequence of reducing Arctic ice cover: Arrival of the Pacific diatom Neodenticula seminae in the North Atlantic for the first time in 800000 years. *Global Change Biology*, *13*, 1910–1921.
Rudels, B. (2015). Arctic Ocean circulation, processes and water masses: A description of observations and ideas with focus on the period prior to the international polar year 2007–2009. *Progress in Oceanography*, *132*, 22–67.
Selkoe, K. A., & Toonen, R. J. (2011). Marine connectivity: A new look at pelagic larval duration and genetic metrics of dispersal. *Marine Ecology Progress Series*, *436*, 291–305.
Shanks, A. L. (2009). Pelagic larval duration and dispersal distance revisited. *The Biological Bulletin*, *216*, 373–385.
Smith, T. M., York, P. H., Broitman, B. R., Thiel, M., Hays, G. C., Van Sebille, E., et al. (2018). Rare long-distance dispersal of a marine angiosperm across the Pacific Ocean. *Global Ecology and Biogeography*, *27*, 487–496.
Steele, M., Morison, J., Ermold, W., Rigor, I., Ortmeyer, M., & Shimada, K. (2004). Circulation of summer Pacific halocline water in the Arctic Ocean. *Journal of Geophysical Research, Oceans*, *109*, n/a–n/a.
Thompson, D. W. J., & Wallace, J. M. (1998). The Arctic oscillation signature in the wintertime geopotential height and temperature fields. *Geophysical Research Letters*, *25*, 1297–1300.
Timmermann, R., Goosse, H., Madec, G., Fichefet, T., Ethe, C., & Dulière, V. (2005). On the representation of high latitude processes in the ORCA-LIM global coupled sea ice–ocean model. *Ocean Modelling*, *8*, 175–201.
Timmermans, M. L., Proshutinsky, A., Golubeva, E., Jackson, J. M., Krishfield, R., Mccall, M., et al. (2014). Mechanisms of Pacific summer water variability in the Arctic's Central Canada Basin. *Journal of Geophysical Research, Oceans*, *119*, 7523–7548.
Treml, E. A., Roberts, J. J., Chao, Y., Halpin, P. N., Possingham, H. P., & Riginos, C. (2012). Reproductive output and duration of the pelagic larval stage determine seascape-wide connectivity of marine populations. *Integrative and Comparative Biology*, *52*, 525–537.
Van Gennip, S. J., Popova, E. E., Yool, A., Pecl, G. T., Hobday, A. J., & Sorte, C. J. B. (2017). Going with the flow: The role of ocean circulation in global marine ecosystems under a changing climate. *Global Change Biology*, *23*, 2602–2617.
Van Herwerden, L., Mcilwain, J., Al-Oufi, H., Al-Amry, W., & Reyes, A. (2006). Development and application of microsatellite markers for *Scomberomorus commerson* (Perciformes; Teleostei) to a population genetic study of Arabian peninsula stocks. *Fisheries Research*, *79*, 258–266.
Van Sebille, E., Griffies, S. M., Abernathey, R., Adams, T. P., Berloff, P., Biastoch, A., et al. (2018). Lagrangian Ocean analysis: Fundamentals and practices. *Ocean Modelling*, *121*, 49–75.
Vermeij, G. J., & Roopnarine, P. D. (2008). The coming Arctic invasion. *Science*, *321*, 780–781.
Wagner, P., Rühs, S., Schwarzkopf, F. U., Koszalka, I. M., & Biastoch, A. (2019). Can Lagrangian tracking simulate tracer spreading in a high-resolution ocean general circulation model? *Journal of Physical Oceanography*, *49*, 1141–1157.
Wang, Q., Ilicak, M., Gerdes, R., Drange, H., Aksenov, Y., Bailey, D. A., et al. (2016). An assessment of the Arctic Ocean in a suite of interannual CORE-II simulations. Part II: Liquid freshwater. *Ocean Modelling*, *99*, 86–109.

Wassmann, P., Kosobokova, K. N., Slagstad, D., Drinkwater, K. F., Hopcroft, R. R., Moore, S. E., et al. (2015). The contiguous domains of Arctic Ocean advection: Trails of life and death. *Progress in Oceanography*, *139*, 42–65.

Webster, M. S., Marra, P. P., Haig, S. M., Bensch, S., & Holmes, R. T. (2002). Links between worlds: Unraveling migratory connectivity. *Trends in Ecology & Evolution*, *17*, 76–83.

Wisz, M. S., Broennimann, O., Grønkjær, P., Møller, P. R., Olsen, S. M., Swingedouw, D., et al. (2015). Arctic warming will promote Atlantic–Pacific fish interchange. *Nature Climate Change*, *5*, 261.

Yaroslavtseva, L. M., & Sergeeva, E. P. (2006). Adaptivity of the bivalve *Mytilus trossulus* larvae to short-and long-term changes in water temperature and salinity. *Russian Journal of Marine Biology*, *32*, 82–87.

Yool, A., Popova, E. E., & Coward, A. C. (2015). Future change in ocean productivity: Is the Arctic the new Atlantic? *Journal of Geophysical Research, Oceans*, *120*, 7771–7790.